Afrika Matematika (2025) 36:84
https://doi.org/10.1007/s13370-025-01292-y

Improved runs-rules precedence charts for monitoring the process location parameter

Schalk William Human[1] · Jean-Claude Malela-Majika[2] · Pierre Kritzinger[3]

Received: 12 September 2024 / Accepted: 12 March 2025
© The Author(s) 2025

Abstract
Runs-rules are typically incorporated into control charts to increase their sensitivity to detect small process shifts. However, a drawback of this approach is that the resulting charts are unable to detect large shifts quickly. In this paper, improved runs-rules are introduced to the nonparametric precedence chart to address this limitation by maintaining the sensitivity to small process shifts, while improving the ability to detect large shifts in the process. Performance comparisons between the proposed precedence charts and the precedence charts with standard runs-rules are made in terms of their respective run-length characteristics. The results reveal that the precedence charts with improved runs-rules are superior to the competing charts in detecting large shifts in the process, while maintaining the same sensitivity in the detection of small shifts. A real-life example from the engineering field is given to demonstrate the application and implementation of the new charts.

Keywords Control chart · False alarm rate · Improved runs-rules · Nonparametric · Precedence · Standard runs-rules

Mathematics Subject Classification 62P30 · 62G30

1 Introduction

Chakraborti et al. [8] proposed the nonparametric Shewhart-type control charts based on the precedence statistic that can be used to monitor any unknown or unspecified (i.e. case U) percentile of a process, this chart is known as the precedence chart. The precedence chart is applied in a setting where no information is available regarding the process. An approach is followed to monitor the process in the so-called Phase I regime. Information regarding the process is gathered in Phase I where the process is in-control (IC). The information that was

✉ Jean-Claude Malela-Majika
malela.mjc@up.ac.za

1 Department of Statistics and Actuarial Science, Stellenbosch University, Private Bag X1, Stellenbosch, South Africa

2 Department of Statistics, University of Pretoria, Lynwood Road, Pretoria 0002, South Africa

3 Independent researcher, 518 Andries Strydom, Waterkloof Glen, Pretoria 0010, South Africa

Published online: 18 April 2025

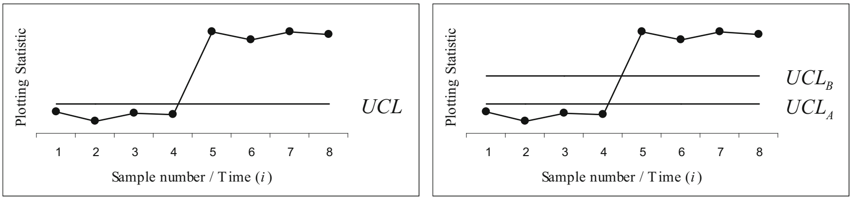

(a) Illustration of an upper one-sided *2-of-2* runs-rules precedence chart

(b) Illustration of an upper one-sided improved *2-of-2* runs-rules precedence chart

Fig. 1 The enhanced and the improved runs-rules precedence chart

gathered in Phase I is then used to monitor the process in the so-called Phase II regime where one is interested in detecting assignable causes in the process.

The precedence chart is based on the classic *1-of-1* signalling rule i.e. the chart signals when the plotting statistic plots on or outside the control limit(s) for the first time and uses only the most recent plotting statistic to determine whether the process is IC or out-of-control (OOC). Hence, the *1-of-1* precedence chart (or basic precedence chart) is known to be relatively insensitive to small process shifts (see e.g. Klein [17], Chakraborti et al. [3] and Malela-Majika and Graham [4]). Chakraborti et al. [3] addressed this shortcoming of the *1-of-1* precedence chart by introducing several runs-type rules such as the *2-of-2* and *2-of-3* runs-rules and showed that their "runs-rules enhanced" precedence charts outperform the *1-of-1* precedence chart. Similar rules have been recently discussed by Chong et al. [5, 7] and Panayiotou and Triantafyllou [6]. Chong et al. [5, 7] demonstrated the superiority of the 2-*of*-3 runs-rules charts over those without runs-rules.

Since standard runs-rules enhanced control charts need more than one plotting statistic to be examined (e.g. the *2-of-2* runs-rule needs two plotting statistics), they are not as good at quickly detecting large shifts. As an illustration, consider the upper one-sided *2-of-2* runs-rules enhanced precedence chart illustrated in panel (a) of Fig. 1. Note that even though there seems to be a substantial assignable cause present in the process from the fifth time point, the chart only signals at the sixth time point, upon plotting of the sixth plotting statistic above the UCL. To remedy this, a second upper control limit can be introduced, namely, UCL_B, above the UCL, and the new chart is set to signal as soon as a single plotting statistic plots on or above UCL_B or if any two consecutive plotting statistics plot on or above the UCL. Note that the new chart uses two (upper) control limits, one, the UCL_B and the other, the UCL_A, which is taken to be the same as UCL, the upper control limit associated with the *2-of-2* runs-rules precedence chart. Hence, the new chart is expected to be as sensitive as the *2-of-2* runs-rules precedence chart for detecting small process shifts but more sensitive to larger shifts. This new chart, called the upper one-side improved *2-of-2* runs-rules precedence chart is shown in panel (b) of Fig. 1, then signals on the fifth plotting statistic. Other examples can be given where one may have to wait for a much longer length of time before the *2-of-2* chart signals. Adding the proposed improved runs-rules can significantly reduce the waiting time to a signal when there is indeed a large process change.

Improved runs-rules are then described as the combination of the basic 1-*of*-1 run-rule and the standard runs-rules. The term "improved" indicates the superiority of the resulting rule over the standalone 1-*of*-1 and standard runs-rules; see for example, Khoo and Ariffin [16] and Malela-Majika et al. [15]. Khoo and Ariffin [16] introduced the improved runs-rules to the Shewhart-type $\overline{X}$ chart and showed that the resulting chart outperforms the $\overline{X}$

chart with runs-rules considered by Klein [17]. Similarly, Kritzinger et al. (2012) introduced the improved runs-rules to the Sign chart and showed that the resulting chart outperforms the Sign chart with runs-rules proposed by Human et al. (2010). Malela-Majika et al. [21] and (2016b) proposed the precedence and Mann–Whitney control charts with supplementary improved runs-rules, respectively. The charts supplemented with improved runs-rules were reported to be superior to the ones with standard runs-rules. The results from this study lends support towards the improved runs-rules precedence charts as they are seen to be superior in detecting larger process shifts, while maintaining the same sensitivity as the runs-rules in the detection of small shifts. Note that for the improved runs-rules sign chart the range of possible IC value combinations is a challenge due to the discreteness of the plotting statistic. This challenge will be overcome to a large extent in the improved runs-rules precedence charts by choosing the Phase I reference sample sufficiently large. This point will be elaborated on further in this paper.

The rest of this paper is outlined as follows: In Sect. 2, the plotting statistic and important notations of the standard and improved runs-rules precedence charts are introduced. In Sect. 3, a summary of the signalling events is presented. In addition, the formulas that are used to calculate the run-length distribution and some characteristics of the run-length distribution are discussed. The designs of the standard and improved runs-rules precedence control charts are discussed in Sect. 4. In Sect. 5, the performance of the improved runs-rules precedence chart is discussed. In addition, the proposed improved runs-rules precedence chart is compared to the standard runs-rules precedence chart. Finally, in Sect. 6, the summary and conclusions section are provided.

2 Mathematical background

2.1 Assumptions

Suppose that an IC reference sample of size m from Phase I denoted by $(X_1, X_2, ..., X_m)$ is available from an unknown continuous process distribution with an unknown continuous cumulative distribution function (cdf) $F_X(x) = F(x - \theta)$ where θ is the location parameter and F is some continuous cdf with a median of zero. The Phase I reference sample $(X_1, X_2, ..., X_m)$ is used to estimate the control limit(s) for Phase II monitoring.

In Phase II, test samples of size n, denoted by Y_i $(i = 1,2,3,\ldots)$ are sequentially taken at sampling stage (time) i. Each Phase II test sample Y_i is a random sample (rational subgroup) of size $n > 1$ from an unknown continuous distribution with cdf $G_Y(y) = F(y - \theta_i)$ where θ_i is the location parameter of the k^{th} test sample.

It is assumed that the Phase II test samples Y_i $(i = 1,2,3,\ldots)$ are drawn sequentially and independently of one another and from the Phase I reference sample $(X_1, X_2, ..., X_m)$.

2.2 The plotting statistic and control limits

The precedence chart is based on the order statistics. The plotting (or charting) statistic chosen to be used in the precedence chart is the j^{th} $(j = 1,2,3,\ldots,n)$ order statistic from a Phase II test sample.

The monitoring of a process is carried out as follows: (i) In Phase I, an IC reference sample of size m is obtained from which the control limits are estimated. Note that the estimated control limits are order statistic(s) from the Phase I reference sample. (ii) In Phase II, new incoming samples are taken sequentially from the process. For each new incoming sample, a plotting statistic (an order statistic) is calculated/observed at time $i = 1,2, 3, \ldots$, each plotting statistic is then compared to the control limits estimated in Phase I. If a sequence of plotting statistics of interest occurs on the control chart, the chart signals and a search is initiated to determine if an assignable cause is present.

The plotting statistic is denoted by T_i, where T_i at time $i = 1,2, 3, \ldots$ is the j^{th} order statistic from the i^{th} Phase II test sample $(Y_{i1}, Y_{i2}, \ldots, Y_{in})$, $i = 1,2,3,\ldots$ denoted by $Y^i_{(j:n)}$ for $1 \leq j \leq n$. The minimum, median and maximum precedence charts use $j = 1$, $(n+1)/2$ (here n is an odd number) and n, respectively. In this paper, we focus on the median precedence chart.

To find the control limits for Phase II precedence monitoring scheme, the Phase I reference sample of size m is arranged in ascending order given by:

$$X_{(1:m)} < X_{(2:m)} < X_{(3:m)} < \ldots < X_{(m:m)}$$

where $X_{(k:m)}$ denotes the k^{th} order statistic of the reference sample of size m. The control limits for the basic (i.e. *1-of-1*), runs-rules and improved runs-rules precedence charts are order statistics from the Phase I reference sample and they are determined such that the nominal IC average run-length (ARL_0) is closer or equal to some high desired value such as 370 and 500. Therefore, the order statistics $X_{(a:m)}$, $X_{(b:m)}$, $X_{(c:m)}$ and $X_{(d:m)}$, for $1 \leq a \leq b < c \leq d \leq m$ i.e. $X_{(a:m)} \leq X_{(b:m)} < X_{(c:m)} \leq X_{(d:m)}$, denote the control limits of the precedence charts and are given by:

$\widehat{UCL}_B = x_{(d:m)}$, $\widehat{UCL}_A/\widehat{UCL} = x_{(c:m)}$, $\widehat{LCL}_A/\widehat{LCL} = x_{(b:m)}$, and $\widehat{LCL}_B = x_{(a:m)}$.

Note that, for the improved runs-rules precedence charts, $X_{(a:m)} < X_{(b:m)} < X_{(c:m)} < X_{(d:m)}$; however, when $a = b$ and $c = d$, the standard runs-rules, including the *1-of-1* rule, is used.

3 Characteristics of the run-length distribution of the standard and improved runs-rules charts

In this section, a graphical illustration of the improved runs-rules charts is discussed, and important notations are also introduced and discussed. In addition, the transition probability matrices as well as the run-length properties of the charts under consideration are given.

Different zones (or regions) of the charts under consideration are displayed in Fig. 2. Note that throughout this paper the *inner* lower (upper) control limit of the improved runs-rules charts is denoted by $\widehat{LCL}_A$ $\left(\widehat{UCL}_A\right)$ and is taken to be same as the lower (upper) control limit of the standard runs-rules enhanced charts denoted by $\widehat{LCL}$ $\left(\widehat{UCL}\right)$. This is denoted by $x_{(b:m)}$ $\left(x_{(c:m)}\right)$ as shown in Fig. 2. The motivation for introducing a second set of control limits is as follows: Standard runs-rules are introduced to improve a chart's efficiency in detecting small shifts by narrowing the control limits while maintaining a sufficiently large IC *ARL*. However, the chart is then unable to detect large shifts quickly, i.e. OOC *ARL* = 1. To address this issue, a second set of control limits is introduced, the inner set of control limits is associated with the runs-rules for increased sensitivity to small shifts and the outer set of control limits makes the chart more sensitive to large shifts.

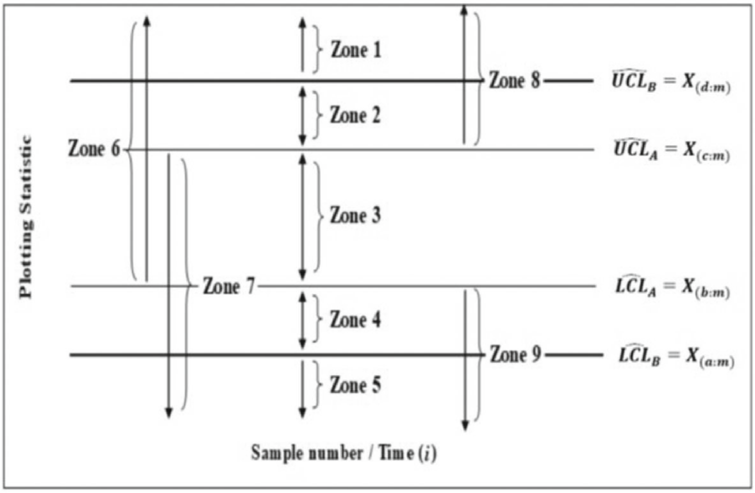

Fig. 2 The different "zones" on the runs-rules and improved runs-rules control charts

Table 1 Notations

Definition of Z_i
$Z_i = 1$ if $\widehat{LCL}_B \leq T_i$
$Z_i = 2$ if $\widehat{UCL}_A \leq T_i < \widehat{UCL}_B$
$Z_i = 3$ if $\widehat{LCL}_A/\widehat{LCL} < T_i < \widehat{UCL}_A/\widehat{UCL}$
$Z_i = 4$ if $\widehat{LCL}_B < T_i \leq \widehat{LCL}_A$
$Z_i = 5$ if $T_i \leq \widehat{LCL}_B$
$Z_i = 6$ if $T_i > \widehat{LCL}_A/\widehat{LCL}$
$Z_i = 7$ if $T_i < \widehat{UCL}_A/\widehat{UCL}$
$Z_i = 8$ if $T_i \geq \widehat{UCL}$
$Z_i = 9$ if $T_i \leq \widehat{LCL}$

It is seen that the four control limits $\widehat{LCL}_B$, $\widehat{LCL}_A$, $\widehat{UCL}_A$ and $\widehat{UCL}_B$ divide the control region into nine "zones". A random variable Z_i is defined according to the zone in which the plotting statistic (T_i) falls. Thus, Z_i takes integer values from 1 to 9, see Table 1.

3.1 Summary of the signalling events

To derive the IC and OOC chart performance properties of the runs-rules control charts, the signalling events of each chart need to be properly defined as the probabilities of these events are the key elements when using the Markov-chain approach. This approach simplifies the approximation of the conditional IC and conditional OOC run-length distribution. Hence, in this section, the signalling events of the *1-of-1*, *2-of-2* and improved *2-of-2* control charts are defined—these events are shown in Table 2.

To explain the notations, consider for example the event $E^1_{1-of-1(U)}$; this is the signalling event of the *1-of-1* upper one-sided control chart. Note the following key elements regarding the notations: (i) The subscripts indicate which run-rule is considered (i.e. the *1-of-1*, *2-of-2*, etc.) and whether it is an upper, lower or a two-sided chart denoted by U, L or T in the brackets, respectively. In this case, the upper one-sided control chart is considered; (ii) The superscript represents the number of the signalling event for each chart; this is necessary because a control chart can have multiple signalling events. In this case, the chart has only a single signalling event, so the superscript can only be 1.

For two additional examples, consider the events $E^2_{2-of-2(T)}$ and $E^3_{I2-of-2(L)}$. The former denotes the second signalling event of the two-sided *2-of-2* chart; whereas, the latter denotes the third signalling event of the lower one-sided improved *2-of-2* chart. Note that the uppercase letter *I* appearing at the beginning of the subscript indicates that the improved chart's signalling event is considered.

3.2 Run-length distribution of the precedence charts

A Markov chain approach and expectation by conditioning is used to obtain the expressions for the IC and OOC run-length distribution. The conditional essential transition probability matrices of all the control charts are given and the formulas that are used to calculate the elements i.e., the transition probabilities, of the conditional essential transition probability matrices are explained.

3.2.1 Transition probabilities

An element inside a conditional essential transition probability matrix is associated with the probability of the plotting statistic T_i plotting inside a "zone" on the control chart given a set of Phase I estimated control limits. The probabilities $p_{iC},\ i = 1{,}2, ..., 9$ are required to set up the conditional essential transition probability matrices.

$p_{1C}, p_{2C}, ..., p_{9C}$ are conditional transition probabilities, conditioned on estimated control limits from Phase I. There are a couple of results needed to calculate the conditional transition probabilities.

Let $Y^i_{(j:n)}$ denote the j^{th} order statistic of the i^{th} Phase II test sample of size n. The probabilities that T_i plots in zones 1, 2, 3, …, 9 can be found using the probability integral transformation. For instance, the probability that T_i plots in zones 1 and 2 are given by

$$\begin{aligned} p_{1C} &= P\left(Y^i_{(j:n)} \geq X_{(d:m)} | X_{(d:m)} = x_{(d:m)}\right) \\ &= 1 - P\left(Y^i_{(j:n)} < X_{(d:m)} | X_{(d:m)} = x_{(d:m)}\right) \\ &= P\left(U_{(j:n)} < GF^{-1}\left(U_{(d:m)}\right) | U_{(d:m)} = u_{(d:m)}\right) \\ &= 1 - (B(j, n-j+1))^{-1} \int_0^{GF^{-1}(u_{(d:m)})} w^{j-1}(1-w)^{n-j} dw \end{aligned}$$

and

$$p_{2C} = P(X_{(c:m)} \leq Y_{(j:n)} < X_{(d:n)} | X_{(c:m)} = x_{(c:m)}, X_{(d:m)} = x_{(d:m)})$$

Table 2 Signalling events of the *1-of-1*, standard and improved *2-of-2* runs-rules control charts

Type of chart	*1-of-1* run-rule	Standard *2-of-2* runs-rules	Improved *2-of-2* runs-rules
Upper one-sided	$E^1_{1-of-1\,(U)} = \{Z_i = 8\}$	$E^1_{2-of-2\,(U)} = \{Z_{i-1} = 8,\ Z_i = 8\}$	$E^1_{I2-of-2\,(U)} = \{Z_i = 1\}$ or $E^2_{I2-of-2\,(U)} = \{Z_{i-1} = 2,\ Z_i = 2\}$
Lower one-sided	$E^1_{1-of-1\,(L)} = \{Z_i = 9\}$	$E^1_{2-of-2\,(L)} = \{Z_{i-1} = 9,\ Z_i = 9\}$	$E^1_{I2-of-2\,(L)} = \{Z_i = 5\}$ or $E^2_{I2-of-2\,(L)} = \{Z_{i-1} = 4,\ Z_i = 4\}$
Two-sided	$E^1_{1-of-1\,(T)} = \{Z_i = 8\}$ or $E^2_{1-of-1\,(T)} = \{Z_i = 9\}$	$E^1_{2-of-2\,(T)} = \{Z_{i-1} = 8,\ Z_i = 8\}$ or $E^2_{2-of-2\,(T)} = \{Z_{i-1} = 9,\ Z_i = 9\}$	$E^1_{I2-of-2\,(T)} = \{Z_i = 1\}$ or $E^2_{I2-of-2\,(T)} = \{Z_{i-1} = 2,\ Z_i = 2\}$ or $E^3_{I2-of-2\,(T)} = \{Z_i = 5\}$ or $E^4_{I2-of-2\,(T)} = \{Z_{i-1} = 4,\ Z_i = 4\}$

$$
\begin{aligned}
&= P(Y_{(j:n)} < X_{(d:m)}|X_{(d:m)} = x_{(d:m)}) - P(Y_{(j:n)} < X_{(d:m)}|X_{(d:m)} = x_{(d:m)}) \\
&= P\big(U_{(j:n)} < GF^{-1}(U_{(d:m)})\big|U_{(d:m)} = u_{(d:m)}\big) - P(U_{(j:n)} \\
&< GF^{-1}(U_{(c:m)})|U_{(c:m)} = u_{(c:m)}) \\
&= (B(j, n-j+1))^{-1}\Bigg(\int_0^{GF^{-1}(u_{(d:m)})} w^{j-1}(1-w)^{n-j}dw \\
&\quad - \int_0^{GF^{-1}(u_{(c:m)})} w^{j-1}(1-w)^{n-j}dw\Bigg),
\end{aligned}
$$

respectively; where $B(j, n-j+1)$ is the standard beta function and the j^{th} order statistic from a sample size of $n(>0)$ from an $Uniform(0{,}1)$ distribution follows a beta distribution with parameters j and $n-j+1$.

Note that the expressions of p_{3C}, p_{4C}, ... and p_{9C} can be derived in a similar manner.

3.2.2 Conditional essential transition probability matrices

This section provides the guidelines on how to obtain the conditional essential transition probability matrices (TPM) of the existing and proposed runs-rules charts. For illustrative purposes, we discuss how to construct the upper one-sided improved *v-of-v* runs-rules chart when $v = 2$ which is also known as the *1-of-1* or *2-of-2* control chart.

To construct any TPM, we need to define the compound pattern denoted as Λ which contains all possible ways of getting the OOC signal. Let assume the values 1, 2 and 7, associated with the plotting statistic T_i falling in zones 1, 2 and 7, respectively. For example, the element '12' indicates that in a sequence of two samples, the first plots in zone 1 and the second in zone 2. Thus, the conditional TPM of the upper one-sided improved *2-of-2* chart is constructed as follows:

Step 1: List all the elements of the compound pattern, i.e. $\Lambda = \{1{,}22\}$.
Step 2: List all the non-absorbing state (or basic transient sub-patterns), i.e. $\eta = \{7{,}2\}$.
Step 3: Introduce a dummy state ϕ showing that the process starts IC.
Step 4: Combine the states found in Steps 1 to 4 to get the state space (denoted as Ω) of the Markov chain representing the set of all possible states, i.e. $\Omega = \{\phi{,}7{,}2{,}1{,}22\}$.
Step 5: Construct the TPM of the upper one-sided improved *2-of-2* chart as follows:

$$
M = \begin{bmatrix} \boldsymbol{Q}_{3\times 3} & \vdots & \boldsymbol{C}_{3\times 2} \\ \cdots & \cdots & \cdots \\ 0_{2\times 3} & \vdots & \boldsymbol{I}_{2\times 2} \end{bmatrix} =
$$

	ϕ	7	2	1	22
ϕ	$p_{\phi,\phi}$	$p_{\phi,7}$	$p_{\phi,2}$	$p_{\phi,1}$	$p_{\phi,22}$
7	$p_{7,\phi}$	$p_{7,7}$	$p_{7,2}$	$p_{7,1}$	$p_{7,22}$
2	$p_{2,\phi}$	$p_{2,7}$	$p_{2,2}$	$p_{2,1}$	$p_{2,22}$
1	$p_{1,\phi}$	$p_{1,7}$	$p_{1,2}$	$p_{1,1}$	$p_{1,22}$
22	$p_{22,\phi}$	$p_{22,7}$	$p_{22,2}$	$p_{22,1}$	$p_{22,22}$

Hence, the conditional essential TPM of the improved *2-of-2* upper one-sided chart $Q_{I2-of-2(U)}^{Con(h\times h)}$ is given by.

$$\boldsymbol{Q}_{I2-of-2(U)}^{Con\ (3\times 3)} = \begin{bmatrix} 0 & p_{7C} & p_{2C} \\ 0 & p_{7C} & p_{2C} \\ 0 & p_{7C} & 0 \end{bmatrix}.$$

The conditional TPM of the *1-of-1* and *2-of-2* standard runs-rules charts can also be constructed in a similar way. The conditional essential TPM of the lower, upper and two-sided precedence charts are provided in Table 3.

The above conditional matrices are very important in the derivation of closed-form expressions of the conditional run-length distribution as well as some associated conditional characteristics. In the next section, these expressions are presented in matrix form for simplicity.

3.2.3 Conditional run-length distribution and various conditional run-length characteristics

The probability density function (pdf), cdf, expected value and variance of the conditional run-length distribution of the control charts under consideration are given by

$$P_C(N = j) = P(N = j|Z = z) = \xi(Q^{Con})^{(j-1)}(I - Q^{Con})1, \text{ for} i = 1, 2, 3, ... \quad (1)$$

$$P_C(N \le j) = P(N \le j|\boldsymbol{Z} = z) = 1 - \boldsymbol{\xi}\left(\boldsymbol{Q}^{Con}\right)^j 1, \quad j = 1, 2, 3, ... \quad (2)$$

$$CARL = E_C(N) = E(N|Z = z) = \xi(I - Q^{Con})^{(-1)}1, \quad (3)$$

and

$$\begin{aligned} CVRL &= VRL_C(N) = VRL(N|Z = z) \\ &= \xi(I + Q^{Con})(I - Q^{Con})^{(-2)}\mathbf{1} - (\xi(I - Q^{Con})^{(-1)}\mathbf{1})^2, \end{aligned} \quad (4)$$

respectively, where $\left(\boldsymbol{Q}^{Con}\right)^0 = \boldsymbol{I}$, $\boldsymbol{Q}^{Con}$ is an $h \times h$ conditional essential transition probability matrix for a given chart, $\boldsymbol{\xi} = \boldsymbol{\xi}_{1\times h} = (1,0, 0, ..., 0)$, $1 = 1_{h\times 1} = (1,1, 1, ..., 1)^T$ and $\boldsymbol{I} = \boldsymbol{I}_{h\times h}$ is the identity matrix. The variable N denotes the run-length random variable and h is an integer value representing the number of transient states.

Thus, the conditional run-length distribution and various conditional associated characteristics of a chart under consideration can be calculated using Eqs. (1), (2), (3) and (4) and by entering the probabilities p_{1C}, p_{2C}, ..., p_{9C} into the corresponding conditional essential transition probability matrix (shown in Table 3). For additional and more general elaborations on (1), (2), (3) and (4), readers are referred to Fu and Lou [9] and Fu et al. [10].

3.2.4 False alarm rates

The false alarm rate (*FAR*) is the probability that a chart signals when the process is IC. The formula for the *FAR* of each chart is presented in Table 4 where the probabilities p_{1C}, p_{2C}, ..., p_{8C} and p_{9C} are determined as explained in Sect. 3.2.1.

Table 3 Conditional Essential Transition Probability Matrices

Type of chart	*1-of-1* run-rule	Standard *2-of-2* runs-rules	Improved *2-of-2* runs-rules
Upper one-sided	$\boldsymbol{Q}_{1-of-1(U)}^{Con\ (2\times2)} = \begin{bmatrix} 0 & p_{7C} \\ 0 & p_{7C} \end{bmatrix}$	$\boldsymbol{Q}_{2-of-2(U)}^{Con\ (3\times3)} = \begin{bmatrix} 0 & p_{7C} & p_{8C} \\ 0 & p_{7C} & p_{8C} \\ 0 & p_{7C} & 0 \end{bmatrix}$	$\boldsymbol{Q}_{I2-of-2(U)}^{Con\ (3\times3)} = \begin{bmatrix} 0 & p_{7C} & p_{2C} \\ 0 & p_{7C} & p_{2C} \\ 0 & p_{7C} & 0 \end{bmatrix}$
Lower one-sided	$\boldsymbol{Q}_{1-of-1(L)}^{Con\ (2\times2)} = \begin{bmatrix} 0 & p_{9C} \\ 0 & p_{9C} \end{bmatrix}$	$\boldsymbol{Q}_{2-of-2(L)}^{Con\ (3\times3)} = \begin{bmatrix} 0 & p_{6C} & p_{9C} \\ 0 & p_{6C} & p_{9C} \\ 0 & p_{6C} & 0 \end{bmatrix}$	$\boldsymbol{Q}_{I2-of-2(L)}^{Con\ (3\times3)} = \begin{bmatrix} 0 & p_{6C} & p_{4C} \\ 0 & p_{6C} & p_{4C} \\ 0 & p_{6C} & 0 \end{bmatrix}$
Two-sided	$\boldsymbol{Q}_{1-of-1(T)}^{Con\ (2\times2)} = \begin{bmatrix} 0 & p_{3C} \\ 0 & p_{3C} \end{bmatrix}$	$\boldsymbol{Q}_{2-of-2(T)}^{Con\ (4\times4)} = \begin{bmatrix} 0 & p_{3C} & p_{8C} & p_{9C} \\ 0 & p_{3C} & p_{8C} & p_{9C} \\ 0 & p_{3C} & 0 & p_{9C} \\ 0 & p_{3C} & p_{8C} & 0 \end{bmatrix}$	$\boldsymbol{Q}_{I2-of-2(T)}^{Con\ (4\times4)} = \begin{bmatrix} 0 & p_{3C} & p_{2C} & p_{4C} \\ 0 & p_{3C} & p_{2C} & p_{4C} \\ 0 & p_{3C} & 0 & p_{4C} \\ 0 & p_{3C} & p_{2C} & 0 \end{bmatrix}$

Table 4 The Conditional *FAR* of the *1-of-1*, standard and improved *2-of-2* runs-rules control charts

	Time (i)	*FAR* of the *1-of-1* charts	*FAR* of the *2-of-2* charts	*FAR* of the improved *2-of-2* charts
Upper one-sided	1	$(p_{8C}\|G = F)$	0	$(p_{1C}\|G = F)$
	2,3,4…	$(p_{8C}\|G = F)$	$\left((p_{8C})^2\|G = F\right)$	$\left(p_{1C} + p_{2C}{}^2\|G = F\right)$
Lower one-sided	1	$(p_{9C}\|G = F)$	0	$(p_{5C}\|G = F)$
	2,3,4…	$(p_{9C}\|G = F)$	$\left((p_{9C})^2\|G = F\right)$	$\left(p_{5C} + p_{4C}{}^2\|G = F\right)$
Two-sided	1	$(p_{8C} + p_{9C}\|G = F)$	0	$(p_{1C} + p_{5C}\|G = F)$
	2,3,4…	$(p_{8C} + p_{9C}\|G = F)$	$\left((p_{8C})^2 + (p_{9C})^2\|G = F\right)$	$\left(p_{1C} + p_{5C} + p_{2C}^2 + p_{4C}^2\|G = F\right)$

3.2.5 Unconditional run-length distribution and some unconditional run-length characteristics of the two-sided *1-of-1* precedence chart

The unconditional run-length distribution and some characteristics of the unconditional run-length distribution of the two-sided *1-of-1* precedence chart are given by:

$$P\left(N_{1-of-1(T)} = j\right) = \int_0^1\int_0^{\kappa} P_C\left(N_{1-of-1(T)} = j\right) f_{bc}(\iota,\ \kappa)\, d\iota d\kappa$$
$$= \int_0^1\int_0^{\kappa} \boldsymbol{\xi}(\boldsymbol{Q})^{j-1}(\boldsymbol{I}-\boldsymbol{Q})\, 1\ f_{bc}(\iota,\ \kappa)\, d\iota d\kappa \tag{5}$$

$$ARL_{1-of-1(T)} = \int_0^1\int_0^{t} CARL_{1-of-1(T)}\ f_{bc}(s,\ t)\, dsdt$$
$$= \int_0^1\int_0^{t} \boldsymbol{\xi}(\boldsymbol{I}-\boldsymbol{Q})^{-1} 1\ f_{bc}(s,\ t)\, dsdt \tag{6}$$

$$\begin{aligned} VRL_{1-of-1(T)} &= \int_0^1\int_0^{t} CVRL_{1-of-1(T)} f_{bc}(s,\ t) dsdt \\ &+ \int_0^1\int_0^{t} \left(CARL_{1-of-1(T)}\right)^2 f_{bc}(s,\ t) dsdt \\ &- \left(\int_0^1\int_0^{t} CARL_{1-of-1(T)} f_{bc}(s,\ t) dsdt\right)^2 \\ &= \int_0^1\int_0^{t}\left(\boldsymbol{\xi}(\boldsymbol{I}+\boldsymbol{Q})(\boldsymbol{I}-\boldsymbol{Q})^{-2}1 - \left(\boldsymbol{\xi}(\boldsymbol{I}-\boldsymbol{Q})^{-1}1\right)^2\right) f_{bc}(s,\ t) dsdt \\ &+ \int_0^1\int_0^{t}\left(\boldsymbol{\xi}(\boldsymbol{I}-\boldsymbol{Q})^{-1}1\right)^2 f_{bc}(s,\ t) dsdt \\ &- \left(\int_0^1\int_0^{t} \boldsymbol{\xi}(\boldsymbol{I}-\boldsymbol{Q})^{-1}1 f_{bc}(s,\ t) dsdt\right) \end{aligned} \tag{7}$$

and

$$FAR_{1-of-1(T)} = \int_0^1\int_0^{t} UFAR_{1-of-1(T)} f_{bc}(s,\ t)\, dsdt$$
$$= \int_0^1\int_0^{t} \left(p_{8C} + p_{9C} | G = F\right) f_{bc}(s,\ t)\, dsdt, \tag{8}$$

where $\boldsymbol{Q} = \boldsymbol{Q}^{Con}$ and $f_{bc}(s,\ t) = \frac{m!}{(b-1)!(c-b-1)!(m-c)!} t^{b-1}(t-s)^{c-b-1}(1-t)^{m-c}$ is the joint pdf of the b^{th} and c^{th} order statistics in a random sample of size m from the Uniform (0,1) distribution.

The expressions for the unconditional run-length distribution and associated unconditional characteristics can be written in a similar format for the upper and lower *1-of-1*, upper, lower and two-sided *2-of-2* and upper, lower and two-sided improved *2-of-2* charts.

In order to apply the charts in practice, the control limits are needed. This is discussed next.

4 Design of the improved runs-rules precedence charts

The background and explicit formulas for the precedence charts have been established. But, what are still lacking are the charting constants for the improved runs-rules precedence charts using the backward approach. Therefore, the order statistics from the IC reference sample need to be established. These order statistics are used as the control limits in Phase II monitoring. This would ensure a chart which has desirable properties.

Note that to calculate the IC and OOC run-length distribution and the characteristics of the improved runs-rules precedence charts are complicated. Solving these equations is resource intensive. The software package Mathcad®14.0 was used in one-sided IC cases, however, the rest was simulated in SAS.

Tables 5 and 6 are constructed by allowing the outer control limit UCL_B to be as large as possible (i.e. making UCL_B as un-influential as possible) while at the same time choosing the inner control limit UCL_A such that the unconditional *ARL* (*UARL*) is as close as possible to 370. The effect is then observed when the outer control limit is gradually brought closer to the UCL_A. From Tables 5 and 6, it can be seen that as the UCL_B is decreased, the *UARL* is at first unaffected, then the *UARL* starts to decrease as expected. Based on the IC performance analysis, when the reference sample size is 100 and 200, the *UARL* is immediately affected as the UCL_B decreases.

There are two motivations for the manner in which Tables 5 and 6 are populated. The first motivation is to limit the combinations of charting constants that need to be investigated since there are many possibilities. The second motivation is that the performance comparisons are simplified since a combination of charting constants can quite easily be found that provide a similar (same) IC *ARL* to the runs-rules enhanced precedence charts.

To illustrate the use of Tables 5 and 6, consider rows 1 to 7 and the far right cells of Table 6. These cells contain the characteristics of the upper one-sided improved *2-of-3* precedence chart when the reference sample is of size 500, the test sample is of size 7 and the 393rd (UCL_A) and 500th (UCL_B) order statistics from the reference sample are used as control limits to monitor the median. Let *FAR*1, *FAR*2, *FAR*234 and *FAR*345 be the unconditional *FAR* for time = 1, time = 2, time = 2, 3, 4,… and time = 3, 4, 5, …, respectively. Then, from the far right cell of the first row of Table 6, the following information can be obtained: $ARL_{I2-of-3(U)} = 361.49$, $FAR1_{I2-of-3(U)} = 0.00000001$, $FAR2_{I2-of-3(U)} = 0.00211750$ and $FAR345_{I2-of-3(U)} = 0.00401624$.

Tables 5 and 6 provide a great deal of information. These tables are of great importance to the quality practitioner in selecting appropriate control limits of the proposed precedence charts.

An example is presented to illustrate the use of Tables 5 and 6 and also the application of the improved runs-rules precedence charts. Thus, Tables 5 displays the unconditional IC *ARL*, unconditional *FAR* at time 1 and 2,3,4, …, and the charting constants (*c*,*d*) for the upper one-sided improved 2-*of*-2 precedence charts for $m \in \{100, 200, 500\}$ and $(n,j) \in \{(5,3), (7,4)\}$. Tables 6 displays the unconditional IC ARL, unconditional FAR at time 1, 2 and 3,4,5, …, and the charting constants (*c*,*d*) for the upper one-sided improved 2-*of*-3 precedence charts for $m \in \{100, 200, 500\}$ and $(n,j) \in \{(5,3), (7,4)\}$.

Remark 1 The precedence statistic is a discrete statistic as the sign statistic i.e. the precedence statistic can only assume a finite number of possible values. Consequently, the precedence chart can only assume a finite number of possible *UARL* and unconditional false alarm rate (*UFAR*) combinations for a choice of *m* and *n*. The possible *UARL* and *UFAR* combinations increases as *m* and *n* increases.

Table 5 Unconditional IC *ARL*, unconditional *FAR* and the charting constants (*c*,*d*) for the upper one-sided improved *2-of-2* precedence chart for $m \in \{100, 200, 500\}$ and $(n,j) \in \{(5,3), (7,4)\}$

	$n=5, j=3$			$n=7, j=4$		
	$m=100$	$m=200$	$m=500$	$m=100$	$m=200$	$m=500$
IC*ARL*	390.45	349.63	365.00	303.91	383.78	352.22
FAR1	0.00005334	0.00000706	0.00000048	0.00000678	0.00000047	0.00000001
FAR234	0.00740930	0.00512795	0.00361770	0.01133275	0.00542242	0.00396963
(*c*,*d*)	(79,100)	(159,200)	(401,500)	(74,100)	(152,200)	(382,500)
IC*ARL*	349.94	317.89	362.08	297.97	377.38	352.05
FAR1	0.00051782	0.00038136	0.00002714	0.00009703	0.00005590	0.00000166
FAR234	0.00778414	0.00544478	0.00363992	0.01140042	0.00546881	0.00397098
(*c*,*d*)	(79,98)	(159,195)	(401,495)	(74,98)	(152,195)	(382,495)
IC*ARL*	281.28	239.06	350.80	279.99	343.08	350.92
FAR1	0.00175854	0.00187392	0.00012313	0.00043158	0.00041777	0.00001206
FAR234	0.00879061	0.00671368	0.00373121	0.01165212	0.00577221	0.00398024
(*c*,*d*)	(79,96)	(159,190)	(401,490)	(74,96)	(152,190)	(382,490)
IC*ARL*	207.78	155.81	328.27	247.96	273.57	347.39
FAR1	0.00409341	0.00514267	0.00038085	0.00123317	0.00152033	0.00004721
FAR234	0.01069985	0.00951387	0.00393757	0.01225836	0.00669983	0.00400990
(*c*,*d*)	(79,94)	(159,185)	(401,485)	(74,94)	(152,185)	(382,485)
IC*ARL*	145.84	96.04	295.51	206.18	191.94	339.70
FAR1	0.00779507	0.01072807	0.00078110	0.00276654	0.00391215	0.00012126
FAR234	0.01376099	0.01435966	0.00430221	0.01342680	0.00872557	0.00407739
(*c*,*d*)	(79,92)	(159,180)	(401,480)	(74,92)	(152,180)	(382,480)
IC*ARL*	100.22	59.64	256.55	162.04	123.96	326.30
FAR1	0.01309294	0.01906042	0.00142281	0.00532072	0.00819766	0.00028059
FAR234	0.01820764	0.02172273	0.00486596	0.01539354	0.01239459	0.00420459
(*c*,*d*)	(79,90)	(159,175)	(401,475)	(74,90)	(152,175)	(382,475)
IC*ARL*	68.99	38.42	216.28	121.91	77.72	306.46
FAR1	0.02017518	0.03046625	0.00233323	0.00919351	0.01498703	0.00049152
FAR234	0.02426358	0.03205126	0.00566744	0.01841729	0.01830187	0.00441737
(*c*,*d*)	(79,88)	(159,170)	(401,470)	(74,88)	(152,170)	(382,470)
IC*ARL*	48.25	25.86	178.61	89.14	49.18	280.67
FAR1	0.02919065	0.04517478	0.00355142	0.01467797	0.02485491	0.00089128
FAR234	0.03214747	0.04578421	0.00674304	0.02277628	0.02708197	0.00474463
(*c*,*d*)	(79,86)	(159,165)	(401,465)	(74,86)	(152,165)	(382,465)

FAR1 = Unconditional false alarm rate *for time* = 1; *FAR234* = Unconditional false alarm rate *for time* = 2, 3, 4…

Table 6 Unconditional IC *ARL*, unconditional *FAR* and the charting constants (*c*,*d*) for the upper one-sided improved *2-of-3* nonparametric chart for $m \in \{100, 200, 500\}$ and $(n,j) \in \{(5,3), (7,4)\}$

	$n=5, j=3$			$n=7, j=4$		
	$m=100$	$m=200$	$m=500$	$m=100$	$m=200$	$m=500$
IC*ARL*	375.52	381.94	363.52	411.00	376.14	361.49
FAR1	0.00005334	0.00000706	0.00000050	0.00000678	0.00000047	0.00000001
FAR2	0.00475813	0.00273040	0.00197355	0.00581425	0.00321304	0.00211750
FAR345	0.00857053	0.00510493	0.00375400	0.01033252	0.00596127	0.00401624
(*c*,*d*)	(81,100)	(164,200)	(412,500)	(77,100)	(156,200)	(393,500)
IC*ARL*	338.19	345.57	360.74	400.34	370.17	361.32
FAR1	0.00051782	0.00038136	0.00002713	0.00009703	0.00005590	0.00000167
FAR2	0.00514999	0.00306232	0.00199661	0.00588790	0.00326143	0.00211895
FAR345	0.00890389	0.00540012	0.00377491	0.01039343	0.00600366	0.00401753
(*c*,*d*)	(81,98)	(164,195)	(412,495)	(77,98)	(156,195)	(393,495)
IC*ARL*	274.41	257.02	349.96	369.79	337.95	360.18
FAR1	0.00175854	0.00187392	0.00012308	0.00043158	0.00041777	0.00001174
FAR2	0.00620188	0.00439138	0.00147987	0.00616174	0.00357775	0.00212855
FAR345	0.00980350	0.00658673	0.00386081	0.01062060	0.00628133	0.00402623
(*c*,*d*)	(81,96)	(164,190)	(412,490)	(77,96)	(156,190)	(393,490)
IC*ARL*	205.20	165.48	328.34	318.77	271.88	356.60
FAR1	0.00409341	0.00514267	0.00038084	0.00123317	0.00152033	0.00004703
FAR2	0.00819648	0.00732316	0.00230506	0.00682091	0.00454512	0.00215932
FAR345	0.01152340	0.00922503	0.00405527	0.01117011	0.00713328	0.00405405
(*c*,*d*)	(81,94)	(164,185)	(412,485)	(77,94)	(156,185)	(393,485)
IC*ARL*	145.82	100.87	296.68	256.43	192.94	348.81
FAR1	0.00779507	0.01072807	0.00078122	0.00276654	0.00391215	0.00012130
FAR2	0.01139276	0.01239353	0.00268312	0.00809038	0.00665666	0.00222954
FAR345	0.01431125	0.01384659	0.00439933	0.01223604	0.00900565	0.00411752
(*c*,*d*)	(81,92)	(164,180)	(412,480)	(77,92)	(156,180)	(393,480)
IC*ARL*	101.26	61.98	258.70	194.59	125.88	335.21
FAR1	0.01309294	0.01906042	0.00142281	0.00532072	0.00819766	0.00028072
FAR2	0.01603250	0.02009117	0.00326737	0.01022504	0.01047909	0.00236197
FAR345	0.01841853	0.02099078	0.00493190	0.01404651	0.01243255	0.00423734
(*c*,*d*)	(81,90)	(164,175)	(412,475)	(77,90)	(156,175)	(393,475)
IC*ARL*	70.18	39.46	219.08	141.53	79.38	315.05
FAR1	0.02017518	0.03046624	0.00233302	0.00919351	0.01498703	0.00049145
FAR2	0.02234616	0.03087704	0.00409792	0.01350283	0.01662884	0.00258325
FAR345	0.02410957	0.03123572	0.00569006	0.01686358	0.01803541	0.00443770
(*c*,*d*)	(81,88)	(164,170)	(412,470)	(77,88)	(156,170)	(393,470)
IC*ARL*	49.21	26.19	181.68	100.38	50.25	288.78

Table 6 (continued)

	$n = 5, j = 3$			$n = 7, j = 4$		
	$m = 100$	$m = 200$	$m = 500$	$m = 100$	$m = 200$	$m = 500$
FAR1	0.02919065	0.04517478	0.00355148	0.01467796	0.02485491	0.00089118
FAR2	0.03055755	0.04519885	0.00521257	0.01822056	0.02576048	0.00292356
FAR345	0.03166874	0.04521988	0.00671165	0.02098636	0.02653684	0.00474606
(*c*,*d*)	(81,86)	(164,165)	(412,465)	(77,86)	(156,165)	(393,465)

FAR1 Unconditional false alarm rate *for time* = 1, *FAR2* Unconditional false alarm rate *for time* = 2, *FAR345* Unconditional false alarm rate *for time* = 3, 4, 5,…

Table 7 Unconditional characteristics of the upper one-sided improved *2-of-2* precedence chart when $m = 125$, $n = 5$ and $j = 3$

I2-of-2(U)				
c	*d*	ARL_0	*FAR1*	*FAR234*
99	125	373.382	0.000028	0.006433
99	124	365.0477	0.000110	0.006500
99	123	350.6366	0.000273	0.006637
99	122	330.4585	0.000539	0.006854
99	121	305.6776	0.000933	0.007178

Example In this example, the inside diameter measurements of forged automobile engine piston rings are monitored using the upper one-sided improved *2-of-2* precedence chart. The IC Phase I reference sample consisting of twenty-five samples of size five each (i.e. a total of 125 observations) given on p.223 in Table 5.3 of Montgomery [18].

To apply the precedence charts the charting constants are required, Table 7 is given to aid in choosing appropriate charting constants.

When constructing a control chart, one typically requires the chart to have a large unconditional IC *ARL*. From Table 7, it can be seen that we found that $c = 99$ and $d = 123$ so that the attained $ARL_0 = 350.64$ for the upper one-sided improved *2-of-2* chart. Therefore, in order to obtain an ARL_0 (unconditional) of 350.64 one need choose the inner and outer upper control limits to be the 99th and 123rd order statistics from the Phase I reference sample of size 125, respectively.

The control limits for the upper one-sided improved *2-of-2* precedence chart are then given by:

$\widehat{UCL}_A = X_{99:125} = 74.009$ and $\widehat{UCL}_B = X_{123:125} = 74.021$

The upper one-sided improved *2-of-2* precedence chart is presented in Fig. 3. The 15 samples from Phase II of size five each are given on page 250 under exercise 5.10 of Montgomery [18].

A plot of the medians is presented in Fig. 3. The first 25 medians are from the IC Phase I reference sample. The last 15 medians are from Phase II monitoring. Considering Fig. 3, the

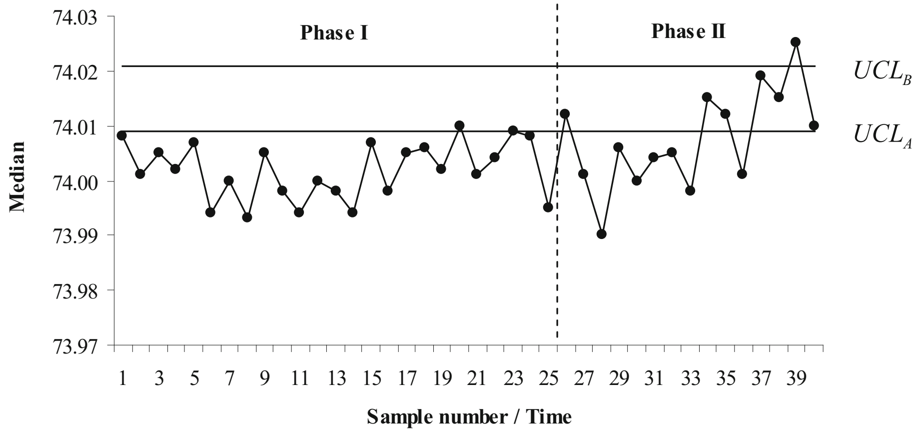

Fig. 3 The upper one-sided improved *2-of-2* precedence chart for the Montgomery [18] piston-ring data

upper one-sided improved *2-of-2* precedence chart detects the first signal at sample number 35 since two consecutive plotting statistics (i.e., 34th and 35th) plotted above the UCL_A.

Note that for the upper one-sided standard *2-of-2* precedence chart, the chart will signal at sample number 35 since two consecutive plotting statistics plotted on or above the UCL_A/UCL. For illustration purposes, assume that the one-sided *1-of-1* precedence chart control limit is equal to UCL_A/UCL, then the chart would signal on the 26th sample since a single plotting statistic plotted above the UCL_A/UCL.

The example illustrates that the application of the improved runs-rules precedence charts is quite simple. The challenge is to determine appropriate charting constants so that the chart has desirable properties.

5 Performance of the standard and improved 2-*of*-2 runs-rules precedence charts

Improved runs-rules are introduced to address a shortcoming of the standard runs-rules charts, namely the inability to detect large shifts quickly. In this section, the performance comparisons between the upper one-sided standard and improved *2-of-2* precedence charts are made.

The performance comparisons between the standard and improved runs-rules precedence charts are done by considering the standard normal (N(0,1), symmetric distribution), Student' s t distribution with v degrees of freedom ($t(v)$, symmetric with heavy tails) and the exponential distribution with parameter λ (*Exp* (λ), positively skewed). It will be shown in the performance analysis that the improved runs-rules precedence charts do not keep the same performance ability under different underlying process distributions.

Tables 8, 9, 10 investigate the performance of the upper one-sided *2-of-2* runs-rules precedence chart under the *Exp*(1), N(0,1), t(4) distributions, respectively. A comparison needs to be done between the upper one-sided standard and improved *2-of-2* runs-rules precedence charts. From Tables 8, 9, 10, it can be seen that the reference sample size is 500 ($m = 500$), the test sample size is 7 ($n = 7$), and the control limits are $UCL_A = 382$ and $UCL_B = 490$. Note that the first column contains the shift in the underlying process distribution (expressed in standard deviation units). In addition, columns two to eight (nine to fifteen) contain the

Table 8 Unconditional characteristics of the upper one-sided standard and improved *2-of-2* runs-rules precedence charts when the underlying process distribution is *Exp*(1)

Exp(1) Distribution ($n = 7, j = 4$, $m = 500$, $c = 382$, $d = 490$)

Shift	*2-of-2* (U)							*I2-of-2* (U)						
	ARL	*IQR*	*5th*	Q_1	*MDRL*	Q_3	*95th*	*ARL*	*IQR*	*5th*	Q_1	*MDRL*	Q_3	*95th*
− 0.05	491.41	511	20	112	284	623	1647	488.34	509	20	111	283	620	1636
0	351.28	363	15	82	205	445	1174	350.52	363	15	81	203	444	1170
0.25	73.98	76	4	19	45	95	240	74.17	77	4	19	45	96	241
0.5	18.95	18	2	6	12	24	58	18.94	18	2	6	12	24	58
0.75	6.33	6	2	2	4	8	17	6.33	6	2	2	4	8	17
1	2.97	2	2	2	2	4	6	2.98	2	2	2	2	4	6
1.25	2.10	0	2	2	2	2	3	2.10	0	2	2	2	2	3
1.5	2.00	0	2	2	2	2	2	2.00	0	2	2	2	2	2
1.75	2.00	0	2	2	2	2	2	1.99	0	2	2	2	2	2
2	2.00	0	2	2	2	2	2	1.98	0	2	2	2	2	2
2.25	2.00	0	2	2	2	2	2	1.95	0	1	2	2	2	2
2.5	2.00	0	2	2	2	2	2	1.89	0	1	2	2	2	2
2.75	2.00	0	2	2	2	2	2	1.78	0	1	2	2	2	2
3	2.00	0	2	2	2	2	2	1.62	1	1	1	2	2	2
3.25	2.00	0	2	2	2	2	2	1.40	1	1	1	1	2	2
3.5	2.00	0	2	2	2	2	2	1.21	0	1	1	1	1	2
3.75	2.00	0	2	2	2	2	2	1.08	0	1	1	1	1	2
4	2.00	0	2	2	2	2	2	1.02	0	1	1	1	1	1

Table 9 Unconditional characteristics of the upper one-sided standard and improved *2-of-2* runs-rules precedence charts when the underlying process distribution is $N(0,1)$

$N(0,1)$ Distribution ($n = 7, j = 4, m = 500, c = 382, d = 490$)

Shift	*2-of-2* (U)							*I2-of-2* (U)						
	ARL	*IQR*	*5th*	Q_1	*MDRL*	Q_3	*95th*	*ARL*	*IQR*	*5th*	Q_1	*MDRL*	Q_3	*95th*
− 0.05	550.30	570	22	124	315	694	1847	547.73	570	22	123	313	693	1852
0	352.38	365	15	81	205	446	1177	353.17	368	15	81	205	449	1177
0.25	53.10	56	4	14	34	70	167	52.75	55	4	14	33	69	167
0.5	13.62	13	2	5	9	18	40	13.53	13	2	5	9	18	39
0.75	5.58	5	2	2	4	7	14	5.53	5	2	2	4	7	14
1	3.27	2	2	2	2	4	7	3.21	2	2	2	2	4	7
1.25	2.44	0	2	2	2	2	4	2.37	0	2	2	2	2	4
1.5	2.14	0	2	2	2	2	3	1.99	0	1	2	2	2	3
1.75	2.04	0	2	2	2	2	2	1.75	1	1	1	2	2	2
2	2.01	0	2	2	2	2	2	1.53	1	1	1	2	2	2
2.25	2.00	0	2	2	2	2	2	1.32	1	1	1	1	2	2
2.5	2.00	0	2	2	2	2	2	1.16	0	1	1	1	1	2
2.75	2.00	0	2	2	2	2	2	1.06	0	1	1	1	1	2
3	2.00	0	2	2	2	2	2	1.02	0	1	1	1	1	1
3.25	2.00	0	2	2	2	2	2	1.01	0	1	1	1	1	1
3.5	2.00	0	2	2	2	2	2	1.00	0	1	1	1	1	1
3.75	2.00	0	2	2	2	2	2	1.00	0	1	1	1	1	1
4	2.00	0	2	2	2	2	2	1.00	0	1	1	1	1	1

Table 10 Unconditional characteristics of the upper one-sided standard and improved 2-of-2 runs-rules precedence charts when the underlying process distribution is $t(4)$

$t(4)$ Distribution ($n = 7, j = 4, m = 500, c = 382, d = 490$)

Shift	*2-of-2* (U)							*I2-of-2* (U)						
	ARL	*IQR*	*5th*	Q_1	*MDRL*	Q_3	*95th*	*ARL*	*IQR*	*5th*	Q_1	*MDRL*	Q_3	*95th*
− 0.05	595.46	616	24	135	342	751	1997	590.72	617	24	133	340	750	1977
0	350.83	364	15	81	205	445	1168	351.52	367	15	81	206	448	1167
0.25	36.84	38	3	10	23	48	115	36.72	38	3	10	23	48	115
0.5	7.98	7	2	3	6	10	22	7.97	7	2	3	6	10	22
0.75	3.45	2	2	2	2	4	8	3.44	2	2	2	2	4	8
1	2.38	0	2	2	2	2	4	2.37	0	2	2	2	2	4
1.25	2.09	0	2	2	2	2	3	2.07	0	2	2	2	2	3
1.5	2.02	0	2	2	2	2	2	1.94	0	1	2	2	2	2
1.75	2.00	0	2	2	2	2	2	1.80	0	1	2	2	2	2
2	2.00	0	2	2	2	2	2	1.58	1	1	1	2	2	2
2.25	2.00	0	2	2	2	2	2	1.35	1	1	1	1	2	2
2.5	2.00	0	2	2	2	2	2	1.16	0	1	1	1	1	2
2.75	2.00	0	2	2	2	2	2	1.06	0	1	1	1	1	2
3	2.00	0	2	2	2	2	2	1.02	0	1	1	1	1	1
3.25	2.00	0	2	2	2	2	2	1.00	0	1	1	1	1	1
3.5	2.00	0	2	2	2	2	2	1.00	0	1	1	1	1	1
3.75	2.00	0	2	2	2	2	2	1.00	0	1	1	1	1	1
4	2.00	0	2	2	2	2	2	1.00	0	1	1	1	1	1

characteristics of the upper one-sided standard runs-rules precedence chart (upper one-sided improved runs-rules precedence chart). Refer to Table 2 for clarity on the notations.

Under the $t(4)$ distribution, it can be observed that when the process is IC, the IC *ARL* values of the upper one-sided standard and improved runs-rules precedence charts are 350.83 and 351.52, respectively. Since the IC *ARL* is the same or approximately so, then the OOC performance comparison analysis is meaningful. Consider an upward shift in the process of 0.25 standard deviation units, then the OOC *ARL* values are 36.84 and 36.72 for the upper one-sided standard and improved *2-of-2* runs-rules precedence charts, respectively (note that the other characteristics are also similar or almost the same). From this, the first claim is supported that for small process shifts, the improved runs-rules precedence charts are as sensitive as the standard runs-rules precedence charts. Now consider an upward shift in the process of 4 standard deviation units, then the OOC *ARL* is 2 and 1.00 for the upper one-sided standard and improved *2-of-2* runs-rules precedence charts, respectively. From this, the second claim is supported that the improved runs-rules precedence charts detect larger shifts in the process more efficiently. The rest of the findings also confirm the superiority of the improved runs-rules precedence charts in the presence of larger process shifts.

From Tables 8, 9, 10, it can be seen that the upper one-sided improved *2-of-2* precedence chart is as sensitive to small process shifts compared to the upper one-sided *2-of-2* precedence chart, while having the ability to detect large process shifts more efficiently. However, under the $Exp(1)$ distribution for upward shifts, the OOC *ARL* of the upper one-sided improved *2-of-2* precedence chart seems to converge slower to one i.e. less efficient in the detection of large process shifts compared to the $t(4)$ and $N(0,1)$ distributions.

Remark 2 Note that Tables 8, 9, 10 are rich in information regarding the OOC performance of the standard and improved runs-rules precedence charts and each can be an important topic of discussion on their own. However, in this paper, the main concern is to confirm the two claims that the improved runs-rules precedence charts are superior in performance to standard runs-rules precedence charts for large shifts in the process, while maintaining the same sensitivity in the detection of small shifts. These two claims were confirmed in the previous discussion.

The performance comparisons are displayed in Tables 8, 9, 10. The results were obtained by means of computer simulation (250 000 repetitions) using SAS®9.4. Considering Tables 8, 9, 10, it can be seen that the improved runs-rules precedence charts are as sensitive to small process shifts compared to runs-rules precedence charts while having the ability to detect large process shifts quickly.

Remark 3 Note that in order to perform the performance analysis on the precedence charts; a sufficiently large reference sample size is required, so that there exist an outer set of control limits that has an absolute minimal influence on the IC *UARL* of the improved runs-rules precedence charts. This is done so that the IC *UARL* for both standard runs-rules and improved runs-rules precedence charts are almost the same by making sure that the inner set of control limits of the improved runs-rules charts and the control limits of the runs-rules charts are equal. Consequently, the reference sample size is chosen to be 500 in the performance analysis for the upper one-sided improved *2-of-2* runs-rules precedence chart.

Remark 4 The OOC ARL profiles of the standard and improved 2-*of*-2 runs-rules precedence charts for large shifts converge towards 2 and 1, respectively, regardless of the type of distribution. This proves the superiority of the improved 2-*of*-2 runs-rules over the standard 2-*of*-2 runs-rules. In addition, the improved rules enhance significantly the detection ability of the precedence chart in monitoring small to moderate shifts regardless of the type of distribution. Thus, when the detection for small, moderate and large shifts in the location parameter is of interest, practitioners are recommended to use the improved 2-*of*-2 runs-rules precedence chart.

6 Summary and conclusions

Improved runs-rules are introduced to the precedence chart. The run-length distribution of the improved runs-rules precedence charts are derived using a Markov chain approach and conditioning by expectation. The performance analysis is carried out to illustrate that the improved runs-rules precedence charts are superior in performance to standard runs-rules precedence charts for large shifts in the process, while maintaining the same sensitivity in the detection of small shifts.

Note that it may be argued that the improved runs-rules precedence chart is not a significant improvement over the run-rules precedence chart. It may be a valid argument in low value high quantity manufacturing, where a single nonconforming unit is not considered as a significant loss. However, in the manufacturing of costly goods where even a single nonconforming product is considered as a significant loss, the improved runs-rules precedence chart will be valued and considered as a significant improvement by the quality practitioner.

We conclude with a summary of the strengths of the improved runs-rules precedence charts: (1) Do not require a specified underlying process distribution (nonparametric), (2) Do not require the variance of the process to be established, (3) Do not require all observations in each Phase II sample when observations are observed in increasing or decreasing order but only up to the observation/order statistic of interest, (5) Are as sensitive to small process shifts as the existing standard runs-rules based precedence charts but superior in the detection of large process shifts.

In summary, it may be said that the improved runs-rules precedence charts are slightly more complex than the standard runs-rules precedence charts. However, there are rewards in terms of better performance.

In future, researchers can consider enhancing the precedence chart by incorporating improved modified runs-rules to improve its performance at detecting small to large shifts in the location parameter.

Funding Open access funding provided by University of Pretoria. No funds, grants, or other support was received. The authors have no relevant financial or non-financial interests to disclose.

Declarations

Conflict of interest The authors certify that there is no conflict of interest.

Open Access This article is licensed under a Creative Commons Attribution 4.0 International License, which permits use, sharing, adaptation, distribution and reproduction in any medium or format, as long as you give appropriate credit to the original author(s) and the source, provide a link to the Creative Commons licence, and indicate if changes were made. The images or other third party material in this article are included in the article's Creative Commons licence, unless indicated otherwise in a credit line to the material. If material is not included in the article's Creative Commons licence and your intended use is not permitted by statutory regulation or exceeds the permitted use, you will need to obtain permission directly from the copyright holder. To view a copy of this licence, visit http://creativecommons.org/licenses/by/4.0/.

References

1. Amin, R.W., Reynolds, M.R.Jr, Bakir, S.: Nonparametric quality control charts based on the sign statistic. Commun. Stat.-Theory Methods 24(6), 1597–1623 (1995).
2. Champ, C.W., Woodall, W.H.: Exact results for Shewhart control charts with supplementary runs rules. Technometrics **29**(4), 393–399 (1987)
3. Chakraborti, S., Eryilmaz, S., Human, S.W.: A phase II nonparametric control chart based on precedence statistics with runs-type signaling rules. Comput. Stat. Data Anal. **53**(4), 1054–1065 (2009)
4. Malela-Majika, J.-C., Graham, M.A.: Design and comparisons of distribution-free Phase-II charting schemes based on unconditional run-length percentiles. Commun. Stat.-Theory Methods 53(1), 276–293 (2024).
5. Chong, Z.L., Mukherjee, A., Khoo, M.B.C.: Proposed nonparametric runs rules Lepage and synthetic Lepage schemes. Comput. Ind. Eng. **172**, 108217 (2022). https://doi.org/10.1016/j.cie.2022.108217
6. Panayiotou, N.I., Triantafyllou, I.S.: A class of enhanced nonparametric control schemes based on order statistics and runs. Stats **6**, 279–292 (2023). https://doi.org/10.3390/stats6010017
7. Chong, Z.L., Teoh, W.L., Yeong, W.C., Malela-Majika, J.C., Khoo, M.B.: Enhanced distribution-free Cucconi schemes based on runs: an application to the surveillance of daily average customer service time. Comput. Ind. Eng. **197**, 110547 (2024). https://doi.org/10.1016/j.cie.2024.110547
8. Chakraborti, S., Van der Laan, P., Van de Wiel, M.A.: A class of distribution-free control charts". J Royal Stat Society. Series C: Appl. Stat. 53(3), 443–462 (2004).
9. Fu, J.C., Lou, W.Y.W.: Distribution theory of runs and patterns and its applications: a finite Markov chain imbedding approach. World Scientific Publishing Co. Pte. Ltd (2003).
10. Fu, J.C., Spiring, F.A., Xie, H.: On the average run lengths of quality control schemes using a Markov chain approach. Stat. Probab. Lett. **56**, 369–380 (2002)
11. Gibbons, J.D., Chakraborti, S.: Nonparametric statistical inference, 4th edn. Marcel Dekker, New York (2003)
12. Human, S.W., Chakraborti, S., Smit, C.F.: Nonparametric Shewhart-type sign control
13. charts based on runs. Commun. Stat.-Theory Methods 39, 2046–2062 (2010).
14. Human, S.W., Kritzinger, P., Chakraborti, S.: Robustness of the EWMA control chart for individual observations. J. Appl. Stat. **38**(10), 2071–2087 (2011)
15. Malela-Majika, J.-C., Shongwe, S.C., Castagliola, P.: One-sided precedence monitoring schemes for unknown shift sizes using generalized 2-of-(h+1) and w-of-w improved runs-rules. Commun. Stat.-Theory Methods 51(9): 2803–2837 (2022).
16. Khoo, M.B.C., Ariffin, K.N.: Two improved runs rules for the Shewhart X control chart. Qual. Eng. **18**(2), 173–178 (2006)
17. Klein, M.: Two alternatives to the Shewhart X control chart. J. Qual. Technol. **32**(4), 427–431 (2000)
18. Montgomery, D.C.: Introduction to statistical quality control, 5th edition, John Wiley (2005).
19. Page, E.S.: A Modified control chart with warning lines. Biometrica **49**(1/2), 171–176 (1962)
20. Weindling, J.I., Littauer, S.B., De Oliveira, J.T.: Mean action time of the X control chart with warning limits. J. Qual. Technol. **2**(2), 79–85 (1970)
21. Malela-Majika, J.C., Chakraborti, S., Graham, M.A.: Distribution-free Phase II Mann-Whitney control charts with runs-rules. Int. J. Adv. Manufact. Technol. **86**, 723–735 (2016)
22. Malela-Majika, J.C., Chakraborti, S., Graham, M.A.: Distribution-free precedence control charts with improved runs-rules. Appl. Stoch. Models Bus. Ind. **32**(4), 423–439 (2016)

Publisher's Note Springer Nature remains neutral with regard to jurisdictional claims in published maps and institutional affiliations.